A comparison of 200 kN magneto-rheological damper models for use in real-time hybrid simulation pretesting

Article *in* Smart Materials and Structures · May 2011

DOI: 10.1088/0964-1726/20/6/065011

2 authors, including:

Zhaoshuo Jiang
San Francisco State University
70 PUBLICATIONS **428** CITATIONS

SEE PROFILE

Smart Mater. Struct. **20** (2011) 065011 (11pp) doi:10.1088/0964-1726/20/6/065011

A comparison of 200 kN magneto-rheological damper models for use in real-time hybrid simulation pretesting

Z Jiang and R Christenson

Department of Civil and Environmental Engineering, University of Connecticut, 261 Glenbrook Road Unit 2037, Storrs, CT 06279, USA

E-mail: zjiang@engineer.uconn.edu

Received 13 October 2010, in final form 29 March 2011
Published 23 May 2011
Online at stacks.iop.org/SMS/20/065011

Abstract

Control devices can be used to dissipate the energy of a civil structure subjected to dynamic loading, such as earthquake, wave and wind excitation, thus reducing structural damage and preventing failure. The magneto-rheological (MR) fluid damper is a promising device for use in civil structures due to its mechanical simplicity, inherent stability, high dynamic range, large temperature operating range, robust performance, and low power requirements. The MR damper is intrinsically nonlinear and rate dependent. Thus a challenging aspect of applying this technology is the development of accurate models to describe the behavior of such dampers for control design and evaluation purposes. In particular, a new type of experimental testing called real-time hybrid simulation (RTHS) combines numerical simulation with laboratory testing of physical components. As with any laboratory testing, safety is of critical importance. For RTHS in particular the feedback and dynamic interaction of physical and numerical components can result in potentially unstable behavior. For safety purposes, it is desired to conduct pretest simulations where the physical specimen is replaced with an appropriate numerical model yet the numerical RTHS component is left unchanged. These pretest simulations require a MR damper model that can exhibit stability and convergence at larger fixed integration time steps, and provide computational efficiency, speed of calculation, and accuracy during pretest verification of the experimental setup. Several models for MR dampers have been proposed, including the hyperbolic tangent, Bouc–Wen, viscous plus Dahl and algebraic models. This paper examines the relative performance of four MR damper models of large-scale 200 kN MR dampers as needed for pretest simulations of RTHS. Experimental tests are conducted on two large-scale MR dampers located at two RTHS test facilities at the Smart Structures Technology Laboratory at the University of Illinois at Urbana Champaign and the Lehigh University Network for Earthquake Engineering Simulation facility. It is shown that each of the MR damper models examined has relative merits and the ultimate selection of the particular model is dependent on the specific RTHS being tested.

(Some figures in this article are in colour only in the electronic version)

1. Introduction

Structural control shows great potential for reducing vibrations in various civil structures under dynamic loading. Structural control can be classified by the type of device used to impart the control force. The three general classes of structural control devices include passive, active, and semiactive (Spencer and Sain 1997). Semiactive devices may be more appropriate for field applications since semiactive control devices offer the reliability associated with passive control devices, maintain the versatility associated with active control devices and require a low power supply (Spencer and Nagarajaiah 2003).

Numerous semiactive control devices have been proposed for structural control of civil engineering structures. The magneto-rheological (MR) fluid damper appears to be a particularly promising type of semiactive control device (Dyke *et al* 1998, Johnson *et al* 1998, etc). In addition to the controllability, stability (in a bounded-input bounded-output sense), and low power requirements inherent to semiactive devices, MR fluid dampers with their large temperature operating range and relatively small device size have the added benefits of: producing large control forces at low velocities and with very little stiction; possessing a high dynamic range (the ratio between maximum force and minimum force at any given time); and having no moving parts, thus reducing maintenance concerns and increasing the response time (compared to conventional variable-orifice dampers).

Experimental testing is critical in structural dynamics in particular to validate structural control strategies (Housner *et al* 1994). Full-scale experimental verification of structural control is a challenging proposition. The concept of hybrid simulation was proposed and further refined over the past four decades to provide the capability to isolate and only physically test critical components of a structure, while the rest of the structure is simulated numerically in the computer (Hakuno *et al* 1969, Takanashi 1975, Takanashi and Nakashima 1987, Mahin *et al* 1989, Shing *et al* 1996). With the continued advancement of computational technology and hydraulic actuation, a real-time realization of hybrid simulation, called real-time hybrid simulation (RTHS), is now possible to capture the rate-dependent characteristic of physical components (Nakashima 2001). The added benefit of RTHS is that it allows for various damper control strategies and a wide range of system parameters to be examined through the numerical model without modifying the experimental (physical) setup. Recent research on RTHS of MR dampers has been conducted for both small and large-scale MR dampers. Carrion and Spencer (2006, 2007) proposed a model-based feedforward compensator for RHTS and implemented it to evaluate the response of a semiactive control of a structure with an 3 kN MR damper attached. Wu *et al* (2007) proposed an equivalent force control method for solving the nonlinear equations of motion in RHTS and applied it to a single degree-of-freedom structure employing a 100 kN MR damper. Park *et al* (2008) evaluated the seismic performance of a five story building structure equipped with 12 kN MR dampers by using RHTS. Christenson *et al* (2008) and Christenson and Lin (2008) investigated the RTHS experimental setup for multiple 200 kN MR dampers and experimentally verified the performance of the MR dampers as applied to a structure under severe dynamic loading. Chen *et al* (2010) developed an adaptive inverse compensation technique for RTHS and experimentally evaluated the effectiveness of the 200 kN MR dampers for seismic hazard mitigation. Phillips *et al* (2010) proposed a RHTS benchmark study and evaluated different semiactive control strategies for 200 kN MR dampers.

RTHS is a test method that is intrinsically characterized by a balance between system performance and stability. Performance and stability are results of the presence of actuator dynamics in the closed-loop RTHS. Actuator dynamics present themselves in the lower-frequency range as an apparent time delay (Horiuchi *et al* 1996, Carrion and Spencer 2007, Chen and Ricles 2009). The effects of the dynamic interaction and the actuator dynamics is often manifested in steady state or unstable high-frequency oscillations (Kyrychko *et al* 2006). The time delay adds energy into the simulation resulting in system instabilities and potential unstable behavior (Colgate *et al* 1995). The dynamic interaction of the hydraulic actuator and physical component contains a velocity feedback of the hydraulic supply that can affect the performance of the actuator system at the resonant frequencies of the test structure (Dyke *et al* 1995). For highly nonlinear systems, such as MR fluid dampers, the dynamic interaction, while present, is difficult to characterize. To support the RTHS test framework in achieving the appropriate balance of performance and stability, high fidelity models of the physical components, the MR dampers, are developed for pretest simulations of the RTHS system. The use of pretesting, conducting pure simulations of the RTHS test prior to conducting physical tests where the hydraulic actuators and physical components are moved, is a critical step taken at RTHS facilities to insure safety and protect the testing equipment and physical specimens. For RTHS in particular the feedback and dynamic interaction of physical and numerical components can result in potentially unstable behavior. For safety purposes, it is desired to conduct pretest simulations where the physical specimen is replaced with an appropriate numerical model yet the numerical RTHS component is left unchanged. These pretest simulations require accurate models of the physical specimens. The focus of this paper is the evaluation of various MR damper models for use in RTHS pretesting.

This paper examines the relative performance of four MR damper models for large-scale 200 kN MR dampers. The models include a model of the pulse-width modulated (PWM) power amplifier providing current to the damper, a model of the inductance of the large-scale MR dampers coils and surrounding MR fluid as proposed by the authors, and models of the controllable force behavior of the MR damper including hyperbolic tangent, Bouc–Wen, viscous plus Dahl, and a standard algebraic model adapted from literature. Experimental tests of two large-scale 200 kN MR dampers are conducted separately at the Smart Structures Technology Laboratory (SSTL) at the University of Illinois at Urbana Champaign and the Lehigh University Network for Earthquake Engineering Simulation (NEES) facility. The performance of the MR damper models is quantified for stability and convergence, speed of computation, and accuracy. The relative merits of each model for use in RTHS pretesting are discussed and conclusions drawn.

2. Large-scale MR damper

The physical components in this study are large-scale MR dampers used for the seismic protection of a building frame. The large-scale MR dampers are manufactured by the Lord Corporation, which nominally have the same properties, although slight variations in performance have been observed in the system identification testing. A schematic of the

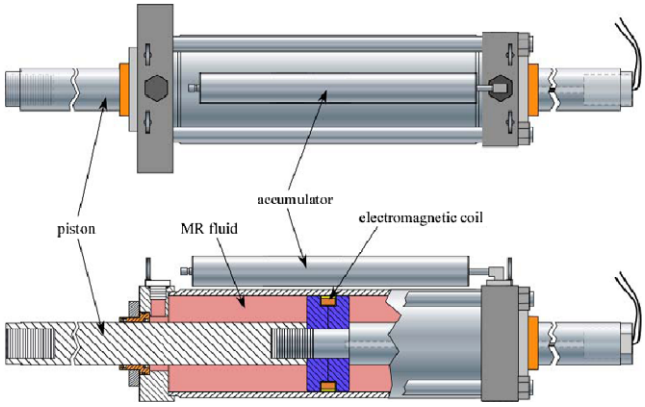

Figure 1. Large-scale semiactive damper schematic.

two large-scale MR dampers used in this study is shown in figure 1. The damper is 1.47 m (58 inches) in length, weighs approximately 2.734 kN (615 lbs), and has an available stroke of 584 mm (23 inches). The damper's accumulator can accommodate a temperature change in the fluid of 80 °F (27 °C). The damper can provide control forces of over 200 kN (45 kip).

The MR damper is controlled with a low voltage, current driven command signal. The coil resistance is approximately 4.8 ohms (Ω), with an associated inductance measured to be approximately 5 henrys (H) at 1 ampere (A) and 3 H at 2 A. An Advanced Motion Controls PWM Servo-Amplifier (30A8DDE) is powered by an 80 volts (V) DC, 5 A unregulated linear power supply. The servo-amplifier is used to provide the command signal that controls the electromagnetic field for each damper. The PWM Servo-Amplifier is controlled by a 0–5 V DC signal and utilizes pulse-width modulation for current control. The input control signal can be switched at a rate up to 1 kHz, although the rise time of the current signal is limited by the inductance of the MR damper. Each damper has been fitted with a 1.5KE75A transient voltage suppressor to protect the MR damper electromagnetic coils from unintended and damaging voltage peaks, limiting the peak voltage to 75 V.

3. Dynamics of variable current

Dynamic response time is an important characteristic for determining the performance of MR dampers in practical civil engineering applications (Yang 2001). For a controllable MR damper the dynamic behavior of not only the MR fluid, but the dynamic response of the current as it is commanded by a particular control law is important. Typically MR damper models are developed and calibrated at constant currents, and so dynamics of the time varying current controlling the dampers must be modeled separately. The PWM amplifier itself and the dynamics of the current in the magnetic coils and surrounding MR fluid of the damper can result in significant reduction in the force response of the MR damper (Jiang and Christenson 2010).

The PWM current driver is represented by a combination of a constant time delay determined to be 0.6 ms and the first order filter:

$$H(s) = \frac{I_{\mathrm{PWM}}}{U} = \frac{1}{1+\tau s} \tag{1}$$

where I_{PWM} is Laplace transform of i_{PWM}, the current produced by the PWM amplifier, U is the Laplace transform of the command signal, u, sent to the PWM amplifier, and the filter time constant τ is determined by experimentally measuring and curve fitting the transfer function between the commanded and measured current to be 3.5 ms.

The magnetic field, and thus the force produced by an MR damper, is directly related to the current in the damper's electromagnetic coil and surrounding MR fluid. The dynamic model of the damper current including the effect of inductance has been developed as

$$G(s) = \frac{I}{I_{\mathrm{PWM}}} = \frac{1}{1+\frac{L}{R}s} \tag{2}$$

where R is resistance of the damper, which is measured as 4.8 Ω, and L is the inductance of the coil and surrounding MR fluid, which is observed to vary as a function of the current as

$$L(t) = \frac{Ri}{\mathrm{d}i/\mathrm{d}t} + L_0 \tag{3}$$

where L_0 is the inductance constant which is chosen as 0.8 H and i is the time varying current.

Details regarding the dynamic models of the current driver and magnetic coils used in this study can be found in Jiang and Christenson (2010).

4. Damper models

Four models are presented here to capture the MR damper force as a function of current and displacement (and velocity) across the damper. These models include the hyperbolic tangent, Bouc–Wen, viscous plus Dahl, and algebraic models.

4.1. Hyperbolic tangent model

The hyperbolic tangent model was proposed by Gavin (2001) for an 8 kN electro-rheological fluid damper. Gavin's model is a simplified version of a system proposed by (Gamota and Filisko 1991). The hyperbolic tangent model used in this research is based on the model proposed by Bass and Christenson (2007). A schematic of this model is shown in figure 2.

As shown in figure 2, the hyperbolic tangent model is composed of two sets of spring–dashpot elements that are connected by an inertial mass element. The inertial mass element resists motion by means of a Coulomb friction element. The displacement and velocity of the inertial mass relative to a fixed based, x_0 and $\dot{x}_0$, and displacement and velocity of damper piston end relative to the inertial mass, x_1 and $\dot{x}_1$, are summed together resulting in the displacement and velocity across the damper, x and $\dot{x}$. The pre-yield visco-elastic behavior is modeled by k_1 and c_1. The post-yield visco-elastic behavior is modeled by k_0 and c_0. The m_0 term represents the inertia of both fluid and the moving piston. The Coulomb friction is a function of the velocity across the element such that $f_0(\dot{x}_0) = f_0 \tanh(\dot{x}_0/V_{\mathrm{ref}})$, where the parameter f_0 is the yield force and V_{ref} is a reference velocity. The dynamics of the

Table 1. Parameters of the hyperbolic tangent model.

Parameters as a function of damper current, i (A)	Units
$k_0 = (0.10i^4 - 1.00i^3 + 1.30i^2 + 2.30i + 6.20) \times 10^{-4}$	kN mm^{-1}
$k_1 = -2.43i^4 + 23.76i^3 - 80.70i^2 + 110.62i + 55.08$	kN mm^{-1}
$c_0 = (-0.98i^4 + 9.33i^3 - 29.96i^2 + 35.80i + 12.64) \times 10^{-2}$	kN s mm^{-1}
$c_1 = (0.62i^4 - 6.73i^3 + 26.69i^2 - 46.06i + 35.67) \times 10^{-2}$	kN s mm^{-1}
$m_0 = (0.16i^4 - 1.62i^3 + 5.48i^2 - 7.05i + 4.85) \times 10^{-3}$	kg
$f_0 = 1.52i^4 - 10.27i^3 + 2.79i^2 + 94.56i + 6.19$	kN
$V_{\text{ref}} = -0.12i^4 + 1.36i^3 - 6.19i^2 + 13.12i + 0.76$	mm s^{-1}

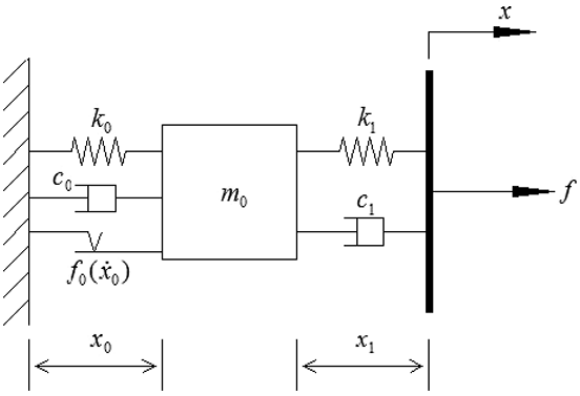

Figure 2. Schematic of the MR damper hyperbolic tangent model.

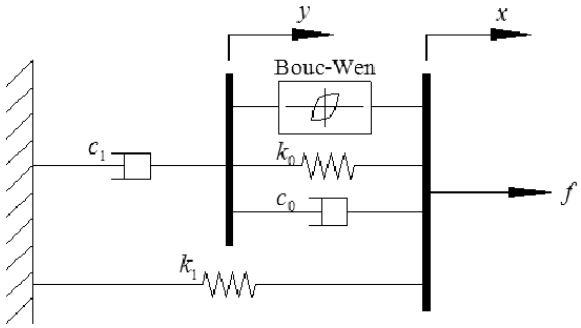

Figure 3. Schematic of the MR damper Bouc–Wen model.

system and force output can be described in state space form as

$$\begin{bmatrix} \dot{x}_0 \\ \ddot{x}_0 \end{bmatrix} = \begin{bmatrix} 0 & 1 \\ (-k_0 - k_1)/m_0 & (-c_0 - c_1)/m_0 \end{bmatrix} \begin{bmatrix} x_0 \\ \dot{x}_0 \end{bmatrix} + \begin{bmatrix} 0 & 0 \\ k_1/m_0 & c_1/m_0 \end{bmatrix} \begin{bmatrix} x \\ \dot{x} \end{bmatrix} + \begin{bmatrix} 0 \\ -1/m_0 \end{bmatrix} \times f_0 \tanh(\dot{x}_0/V_{\text{ref}}) \quad (4)$$

and the MR damper force, f, is a function of the state of equation (4) and the displacement and velocity across the damper as

$$f = \begin{bmatrix} -k_1 & -c_1 \end{bmatrix} \begin{bmatrix} x_0 \\ \dot{x}_0 \end{bmatrix} + \begin{bmatrix} k_1 & c_1 \end{bmatrix} \begin{bmatrix} x \\ \dot{x} \end{bmatrix}. \quad (5)$$

The hyperbolic tangent model requires seven parameters ($k_0, k_1, c_0, c_1, m_0, f_0, V_{\text{ref}}$) to fully characterize the dynamic behavior of the MR damper. The hyperbolic tangent model parameters are determined for fixed sinusoidal displacements and frequency combinations and constant current using a multidimensional unconstrained nonlinear minimization Nelder–Mead direct search simplex method (MathWorks 2007, Lagarias *et al* 1998). The function minimized in this direct search method is the root mean square (RMS) error between the measured and simulated forces over sinusoidal excitations. The values of each model parameter are averaged over the frequency and amplitude for each of the constant current levels identified. Polynomials are fit to the averaged data points for each model parameter as a function of current. Further details on how these parameters are determined can be found in Bass and Christenson (2007). The parameters of the hyperbolic tangent model used in this study are shown in table 1.

4.2. Bouc–Wen model

The Bouc–Wen Model was initially proposed by (Bouc 1971) and generalized by Wen (1976). The Bouc–Wen model used in this study is based on the phenomenological Bouc–Wen model proposed by Spencer *et al* (1997). The model is further modified in this study to accommodate a time varying current. A schematic of the Bouc–Wen model used in this study is shown in figure 3.

In this Bouc–Wen model, the accumulator stiffness is represented by k_1 and the viscous damping observed at larger velocities is represented by c_0. A dashpot, represented by c_1, is included in the model to produce the force roll-off at low velocities which is due to bleed or blow-by of fluid between the piston and the cylinder. k_0 is present to control the stiffness at large velocities, and x_0 is the initial displacement of spring k_1 associated with the nominal damper force due to the accumulator.

The evolutionary variable z is governed by

$$\dot{z} = -\gamma\,|\dot{x} - \dot{y}|\,z|z|^{n-1} - \beta\,(\dot{x} - \dot{y})\,|z|^n + A(\dot{x} - \dot{y}) \quad (6)$$

where

$$\dot{y} = \frac{1}{(c_0 + c_1)}[\alpha z + c_0\dot{x} + k_0(x - y)]. \quad (7)$$

The force output of the MR damper model can be described as

$$f = c_1\dot{y} + k_1\,(x - x_0)\,. \quad (8)$$

This Bouc–Wen model requires ten parameters ($x_0, k_0, k_1, c_0, c_1, \alpha, \beta, \gamma, n, A$) to fully characterize the dynamic behavior of the MR damper. The Bouc–Wen model parameters for constant currents were determined at Lehigh University for a fixed sinusoidal displacement and constant current using

Table 2. Parameters of the Bouc–Wen model.

Parameters as a function of damper current, i (A)	Units
$x_0 = (-0.02i^4 + 0.42i^3 - 3.03i^2 + 0.10i + 165.46) \times 10^{-3}$	m
$k_0 = (-3.55i^4 + 112.58i^3 - 1167.72i^2 + 4257.45i + 100.00) \times 10^{-3}$	kN m^{-1}
$k_1 = (-0.12i^4 + 0.50i^3 + 57.79i^2 - 757.99i + 3039.48) \times 10^{-3}$	kN m^{-1}
$c_0 = -0.04i^4 + 1.43i^3 - 16.47i^2 + 73.67i + 114.43$	kN s m^{-1}
$c_1 = 8.13i^4 - 268.63i^3 + 2987.09i^2 - 12567.09i + 29\,222.96$	kN s m^{-1}
$\alpha = -0.06i^4 + 1.96i^3 - 24.06i^2 + 118.50i + 7.60$	kN m^{-1}
$\beta = (0.31i^4 - 6.65i^3 + 11.76i^2 + 440.62i + 1002.60) \times 10^{-2}$	m^{-2}
$\gamma = 0.10i^4 - 3.11i^3 + 29.16i^2 - 78.44i + 1016.22$	m^{-2}
$n = (-0.171i^4 + 5.75i^3 - 65.50i^2 + 284.59i + 218.47) \times 10^{-2}$	—
$A = -0.15i^4 + 4.44i^3 - 41.64i^2 + 116.95i + 551.21$	—

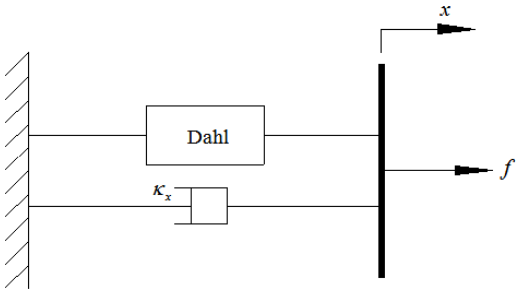

Figure 4. Schematic of the MR damper viscous plus Dahl model.

particle swarm optimization (PSO) approach (Kennedy and Eberhart 1995). The normalized RMS error between the measured and simulated forces sinusoidal excitations was used as the objective function to identify the values of the model parameters. The identified parameters for constant currents are further modified in this research by curve fitting polynomials to provide the model with varying current capacity. The parameters of the Bouc–Wen model used in this study are shown in table 2.

4.3. Viscous plus Dahl

The Dahl model has been proposed independently by Dahl (1968, 1976) to describe frictional behavior, and by Bouc (1971) to represent hysteresis phenomena. The viscous plus Dahl model used in this study is based on the model proposed by Aguirre *et al* (2008). A schematic of viscous plus Dahl model used in this study is shown in figure 4.

The force output of the MR damper model can be described as

$$\dot{w} = \rho(\dot{x} - |\dot{x}|\, w) \tag{9}$$

$$f = \kappa_x \dot{x} + \kappa_w w \tag{10}$$

where w describes the nonlinear behavior of the damper, $\dot{x}$ is the damper piston velocity, κ_x is the viscous friction coefficient and κ_w is the dry friction coefficient. This viscous plus Dahl model requires three parameters (κ_x, κ_w, ρ) to fully characterize the dynamic behavior of the MR damper. The viscous plus Dahl model parameters for constant currents are determined using linear regression analysis. Then polynomials are fit to find the current-dependent parameters. Further details on how these parameters are determined can be found in Aguirre *et al* (2008). The parameters of viscous plus Dahl model used in this study are shown in table 3.

Table 3. Parameters of the viscous plus Dahl model.

Parameters as a function of damper current, i (A)	Units
$\kappa_w = (-1.83i^2 + 11.65i + 0.46) \times 10^4$	N
$\kappa_x = 1.48 \times 10^3$	N s cm^{-1}
$\rho = 0.38 \times 10^2$	cm^{-1}

Table 4. Parameters of the algebraic model.

Parameters as a function of damper current, i (A)	Units
$m = 0.05i + 0.13$	kN s mm^{-1}
$b = -23.40i^2 + 126.52i + 8.18$	kN
$\alpha = 0.15$	s mm^{-1}

4.4. Algebraic model

A nonparametric algebraic modeling technique, or nth order polynomial model, is used to describe the behavior of MR dampers (Choi *et al* 2001, Song *et al* 2005, Ruangrassamee *et al* 2006). In this study, an algebraic model which consists of two components: a polynomial function describing maximum damping force as a function of the control current and a shape function describing the force–velocity dependence has been adopted.

The MR damper force can be described as a linear function of the damper velocity

$$f = \left(1 - \mathrm{e}^{-\alpha|\dot{x}|}\right)(m\,|\dot{x}| + b) \tag{11}$$

where m is the slope and b is the y-intercept parameter which are both observed to be functions of damper current i. An exponential function, with parameter α, is appended to the model to capture the force roll-off at low velocities.

This algebraic model requires three parameters (m, b, α) to fully characterize the dynamic behavior of the MR damper. The algebraic model parameters are determined using regression analysis to minimize the error between measured and predicted force. Details on how these parameters are determined can be found in Ruangrassamee *et al* (2006). The parameters of the algebraic model used in this study are shown in table 4.

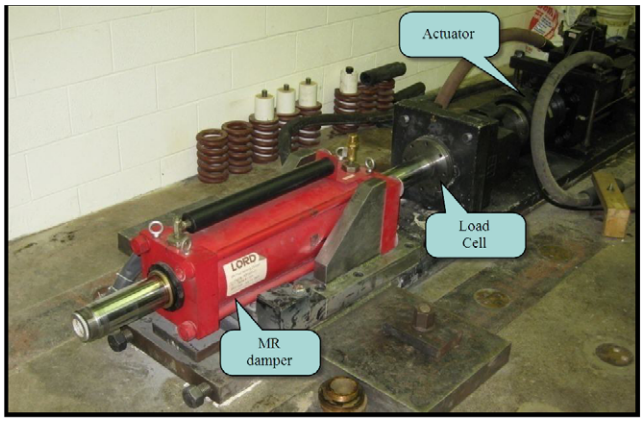

Figure 5. MR damper setup at University of Illinois.

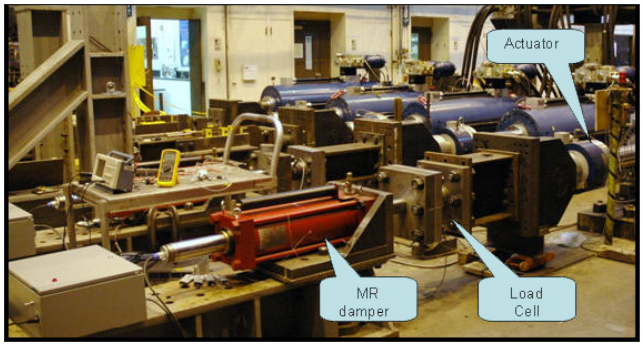

Figure 6. MR damper setup at Lehigh NEES facility.

5. Real-time hybrid simulation

Real-time hybrid tests of the large-scale MR dampers are conducted at the University of Illinois at Urbana Champaign SSTL and at the Lehigh University NEES facility. Different compensation techniques are implemented at the University of Illinois at Urbana Champaign and at the Lehigh University to improve the performance and ensure the stability of RTHS. University of Illinois uses a model-based feedforward–feedback delay compensation technique (Carrion and Spencer 2007) to control a 556 kN hydraulic actuator with 170 mm s^{-1} max velocity. An adaptive compensation method is used to achieve accurate actuator control in a real-time hybrid simulation at Lehigh University (Chen *et al* 2010) to control a 1700 kN hydraulic actuator with 760 mm s^{-1} max velocity. Pictures of the experimental setup for the large-scale MR damper at the University of Illinois and Lehigh University are shown in figures 5 and 6, respectively.

The simulated component of the hybrid test is a benchmark structure proposed by Phillips *et al* (2010). The structure is a three story one bay steel frame building, with total weight of 596 kN. The structure is a linear, in-plane, three degree-of-freedom model with an MR damper attached between the ground and first story as shown in figure 7.

The relative displacement between the ground and first story is assumed to be the displacement across the MR damper. The equation of motion governing the simulated component

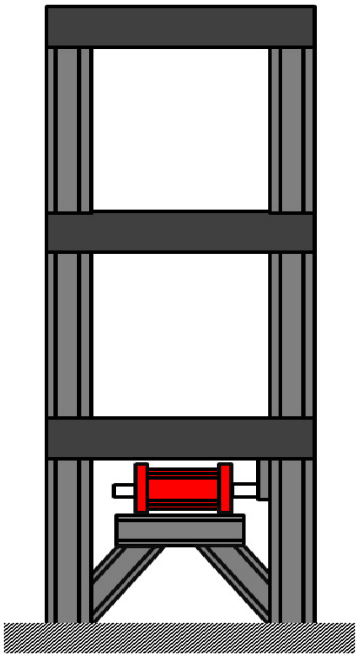

Figure 7. Simulated component—one story one bay frame.

can be represented as

$$\mathbf{M}\ddot{x} + \mathbf{C}\dot{x} + \mathbf{K}x = \mathbf{G}f - \mathbf{M}\mathbf{L}\ddot{x}_g \tag{12}$$

where $x = [x_1 x_2 x_3]^T$ is the relative displacement (x_i) of the ith story, $[\cdot]$ indicates a derivative with respect to time, $\ddot{x}_g$ is the ground acceleration and f is the MR damper force, the mass, **M**, stiffness, **K**, damping, **C**, influence vectors of the MR damper force, **G**, and ground excitation **L** are as:

$$\mathbf{M} = \begin{bmatrix} 20.253 & 0 & 0 \\ 0 & 20.253 & 0 \\ 0 & 0 & 20.253 \end{bmatrix} \times 10^{-3} \text{ kN s}^2 \text{ m}^{-1} \tag{13}$$

$$\mathbf{K} = \begin{bmatrix} 9.933 & -5.662 & 0 \\ -5.662 & 11.340 & -5.662 \\ 0 & -5.662 & 5.662 \end{bmatrix} \text{ kN m}^{-1} \tag{14}$$

$$\mathbf{C} = \begin{bmatrix} 7.243 & -2.069 & 0 \\ -2.069 & 4.139 & -2.069 \\ 0 & -2.069 & 2.069 \end{bmatrix} \times 10^{-3} \text{ kN s m}^{-1} \tag{15}$$

$$\mathbf{G} = \begin{bmatrix} -1 \\ 0 \\ 0 \end{bmatrix} \tag{16}$$

$$\mathbf{L} = \begin{bmatrix} 1 \\ 1 \\ 1 \end{bmatrix}. \tag{17}$$

The natural frequencies of the structure corresponding to the first, second, and third mode are 1.09 Hz, 3.17 Hz, and 4.74 Hz, respectively, with corresponding damping ratios of 0.31%, 0.62%, and 0.63%, respectively, as reported by Carrion and Spencer (2007).

For the semiactive controlled strategy, primary linear quadratic Gaussian (LQG) controller together with a secondary clipped-optimal controller is used to provide the proper current

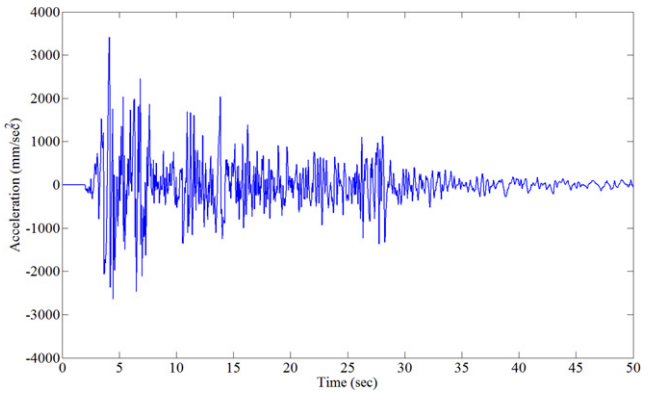

Figure 8. El Centro earthquake record.

level to the damper. This controller uses the clipped-optimal control algorithm with a maximum current of 2.5 A. The LQR gains are selected to achieve optimal response action on force-tracking with $R = 1500$ and $Q = 1$. Further details regarding the control strategy are presented in Phillips *et al* (2010).

The N-S component of the El Centro earthquake recorded at the Imperial Valley Irrigation District substation in El Centro, California, during the Imperial Valley, California earthquake of 18 May 1940, is utilized as the excitation in this study. The earthquake record is shown in figure 8.

6. Performance of MR damper models

The objective of this paper is to examine the relative performance of four identified MR damper models as used for pretest simulations in RTHS testing. The stability and convergence, speed, and accuracy are used here as criteria to evaluate the performance of the damper models in RTHS pretesting. The analytical model results are compared to the University of Illinois experimental results. The experimental results of the real-time hybrid simulations between the Lehigh University and University of Illinois show very close comparison (Phillips *et al* 2010). Lehigh experimental results are compared to University of Illinois experimental results, when applicable, to provide a point of reference to the variability between experimental setups and to allow for the variability in the models to be placed in the proper context.

6.1. Stability and convergence

RTHS systems are generally operated at relatively large numerical integration time step. However, each MR damper model has different requirement on the time step in order to run the simulation stably. Also, different MR damper models have varying range of the time steps to allow the performance to converge. In this portion of the paper, the stability and convergence of the simulations at different numerical time steps is examined. Two error evaluation criteria are used: normalized RMS error of the damper force, as calculated using equation (18) and normalized absorbed energy error as calculated using equation (19). In this study, stability refers to numerical stability of the response from a bounded-input bounded-output sense, while convergence refers to convergence of the normalized performance measured to within 2% of the final value. For all models, a fixed-step explicit fourth order Runge–Kutta numerical integration scheme is used, which is the same as the numerical integration scheme used in the RTHS tests conducted in this paper.

$$\mathrm{Err}_f^{\mathrm{rms}} = \sqrt{\frac{1}{N}\sum_{i=1}^{N}\left[f^{\mathrm{exp}}(t_i) - f^{\mathrm{sim}}(t_i)\right]^2} \Big/ f_{\mathrm{max}}^{\mathrm{exp}} \qquad (18)$$

where f^{exp} and f^{sim} are the damper forces from the physical experiment and from the damper model at time t_i, respectively. $f_{\mathrm{max}}^{\mathrm{exp}}$ is the maximum damper force from the physical experiment.

The energy absorbed by the damper during the seismic event is introduced and used as a means to evaluate the performance of the damper models in this study. The absorbed energy is calculated by summing up the areas under the damper force–displacement curve during an event.

$$\mathrm{Err}^{\mathrm{energy}} = \left|E^{\mathrm{exp}} - E^{\mathrm{sim}}\right| / E^{\mathrm{exp}} \qquad (19)$$

where E^{exp} and E^{sim} the total energy absorbed by the damper in the physical experiment and by the damper model in the pure numerical simulation during an event, respectively.

Figures 9 and 10 show comparison results between different damper models run at different fixed numerical integration time steps. Note that in figures 9 and 10 the normalized RMS errors and normalized absorbed energy errors are further divided by the normalized RMS error and normalized absorbed energy error at time step equal to 1/10 240 (0.0001) respectively to help showing the difference.

The hyperbolic tangent and algebraic damper models are stable up to 12/1024 (0.012) s. The Bouc–Wen damper model becomes unstable when the time step is larger than 11/1024 (0.011) s while the viscous plus Dahl model is unstable at the time step larger than 5/1024 (0.005) s. As can be seen in figure 9, the performance of Bouc–Wen and algebraic models converges for the normalized RMS force error when time step is smaller than 1/1024 (0.001) s while the hyperbolic tangent model performance converges when time step is smaller than 1/2048 (0.0005) s. For the viscous plus Dahl model, the performance becomes consistent when time step is smaller than 1/7168 (0.000 14) s. Since the real-time hybrid simulation are generally run at 1024 Hz, fixed numerical integration time step equal to 1/1024 (0.001) s will be used in the following sections to evaluate these four MR damper models' performance during the RTHS.

6.2. Speed of computation with MR damper models

In RTHS, the numerical portions must be computed within the numerical time step, which requires the MR damper model to be run in a sufficiently small time period. In this portion of the paper, the computational speed of the MR damper models is examined. The simulations of the simulated three story one bay frame shown in above section without any damper attached under a 50 s El Centro earthquake ground excitation stated

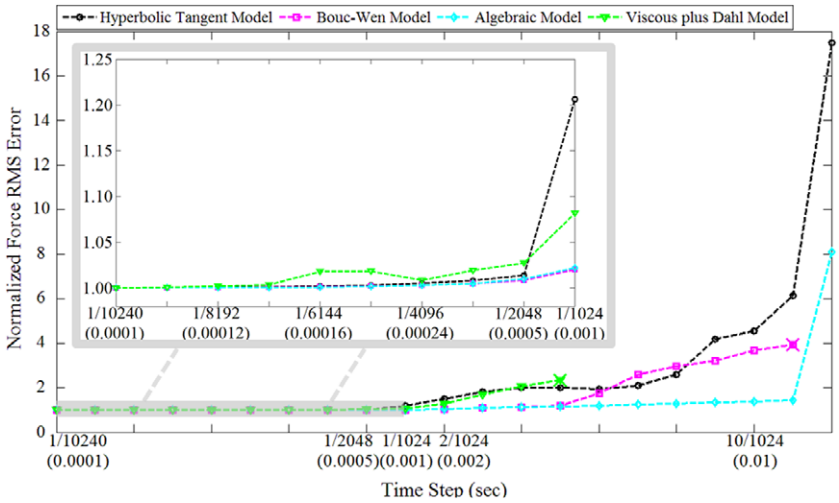

Figure 9. Pure numerical simulation—normalized force RMS error comparison.

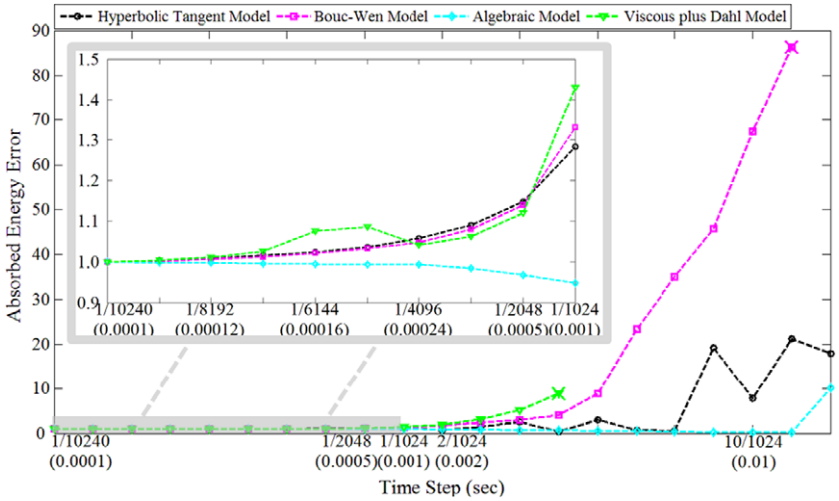

Figure 10. Pure numerical simulation—absorbed energy error comparison.

above and the same building with different damper models attached endured the same earthquake are run for twenty times, respectively. The average run time for each case is calculated and listed in table 5. The variance of twenty run times is smaller than 0.01 s. The normalized run time is then calculated using equation (20) and results are shown in table 5. The computer used to run these tests has an Intel® Core™ 2 Duo T9550 @ 2.66 GHz processor with 4 GB memory running a 32-bit Windows 7 Professional operating system.

$$t^{\text{norm}} = t^{\text{sim}}/t^{\text{total}} \tag{20}$$

where t^{sim} is the average run time for the numerical simulation and t^{total} is the total time of the seismic event.

The algebraic model is fastest requiring 4% normalized run time to compute model. Viscous plus Dahl follows, using 5% normalized run time. The hyperbolic tangent and Bouc–Wen models are about 50% slower, but still sufficiently fast to be used in RTHS pretesting.

Table 5. Speed of different models.

Damper	Simulation run time (s)	Normalized run time (%)
Structure only	0.44	0.88
Structure + hyperbolic tangent	4.22	8.44
Structure + Bouc–Wen	4.43	8.86
Structure + viscous plus Dahl	2.43	4.86
Structure + algebraic	2.10	4.17

6.3. Comparison of damper forces and building responses for numerical simulation and real-time hybrid simulation

Beside the stability, convergence and speed requirements, the accuracy of the numerical portions run at the numerical time step should correspond closely to the ultimate hybrid test in RTHS. In this portion of the paper, the pure numerical simulation results with various damper models are compared to the RTHS results to evaluate the accuracy of the MR damper models. The same fixed-step explicit fourth order Runge–Kutta

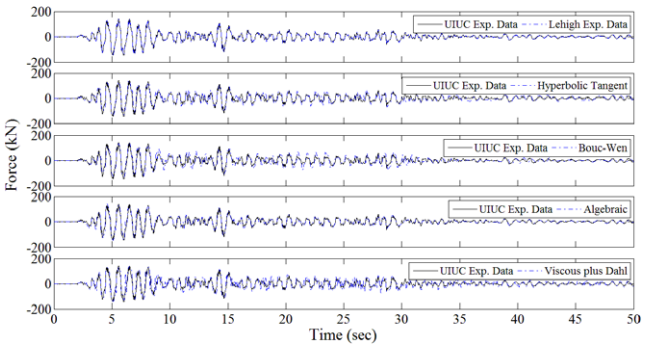

Figure 11. Hybrid testing comparison—force time history.

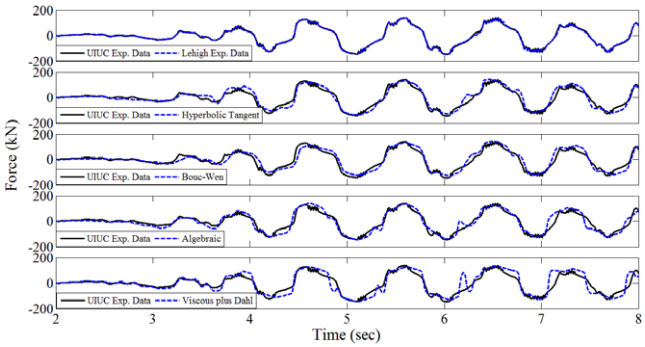

Figure 12. Hybrid testing comparison—force time history (zoom-in).

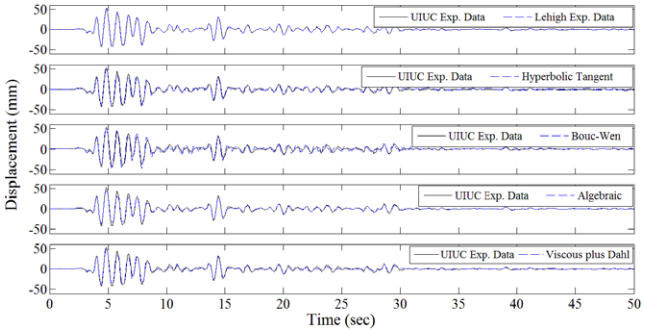

Figure 13. Hybrid testing comparison—1st story displacement comparison.

numerical integration scheme as used in pure simulations is used to solve the equations of motion for in RTHS. Figure 11 shows the force comparison between the different MR damper models and the RTHS results. To highlight the differences more closely, a 6 s portion of the force response is shown in figure 12. The effect of the dynamic interaction and the actuator dynamics is often manifested in steady state or unstable high-frequency oscillations (Kyrychko *et al* 2006) as observed in figure 12 for both UIUC and Lehigh RTHS results. The comparison of the response of the structure for the first story displacement is shown in figures 13 and 14. The first story displacement response represents the response with the greatest disparity between experimental and simulated responses.

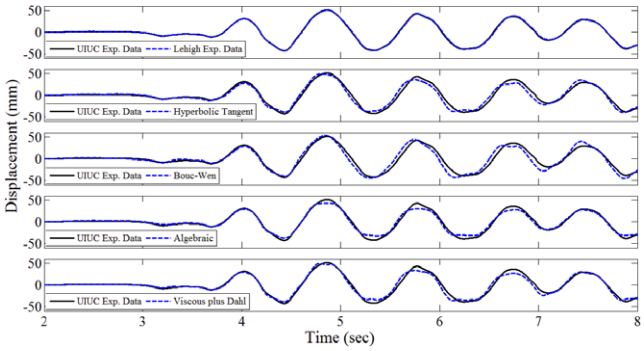

Figure 14. Hybrid testing comparison—1st story displacement comparison (zoom-in).

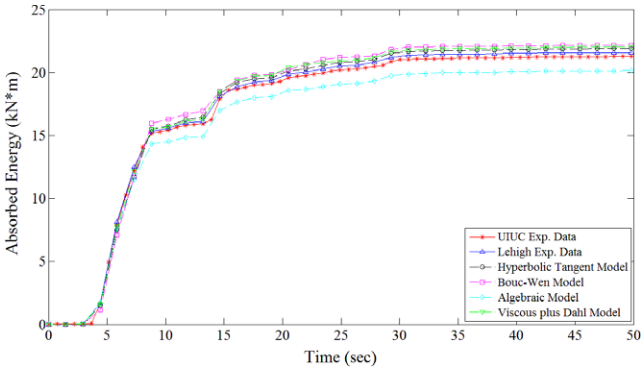

Figure 15. Hybrid testing comparison—absorbed energy comparison.

The comparison of energy absorbed by the different damper models is shown in figure 15.

Besides the normalized force RMS error calculated using equation (18), the normalized displacement RMS error is also calculated using equation (21) and listed in table 6. The error of the absorbed energy is calculated using equation (19) and results are provided in table 6.

$$\mathrm{Err}_x^{\mathrm{rms}} = \sqrt{\frac{1}{N}\sum_{i=1}^{N}\left[x^{\mathrm{exp}}(t_i) - x^{\mathrm{sim}}(t_i)\right]^2} \Big/ x_{\mathrm{max}}^{\mathrm{exp}} \qquad (21)$$

where x^{exp} and x^{sim} are the displacement across the damper from the physical experiment and the damper model at time t_i, respectively. $x_{\mathrm{max}}^{\mathrm{exp}}$ is the maximum displacement across the damper from the physical experiment.

At the time step the real-time hybrid simulations are generally run, 1/1024 (0.001) s, all four models track the experimental data very well. Among those four models, algebraic and hyperbolic tangent model have the best accuracy in terms of normalized force RMS error while Bouc–Wen and viscous plus Dahl follow. As found by Phillips *et al* (2010), the experimental results of the real-time hybrid simulations from the Lehigh University and University of Illinois are very close to each other.

Table 6. Error comparison.

Damper model	First story normalized displacement RMS error (%)	Normalized force RMS error (%)	Absorbed energy (kN m)	Normalized energy error (%)
Hyperbolic tangent	4.67	9.83	22.05	3.63
Bouc–Wen	7.05	13.49	22.15	4.09
Viscous plus Dahl	4.40	13.45	22.04	3.56
Algebraic	3.23	7.93	20.14	5.37
UIUC physical damper	—	—	21.28	—
Lehigh physical damper	0.72	2.85	21.59	1.45

7. Conclusion

By using a simple linear three degree-of-freedom three story single bay model, this paper examines the relative performance of four frequently used damper models, namely the hyperbolic tangent model, Bouc–Wen model, algebraic model and viscous plus Dahl model for RTHS of MR dampers in terms of stability, convergence, speed and accuracy. All four models show good performance and potential in RTHS. It should be noted that there are many factors that have effects on the performance of the models such as different structures, controllers, settings and etc. The following conclusions are based on the specific RTHS experiment examined here.

Regarding to the stability and convergence, the hyperbolic tangent and algebraic damper model can be run stably at up to 12/1024 (0.012) s. Bouc–Wen and viscous plus Dahl damper models require a relatively smaller time step and become unstable at time step larger than 11/1024 (0.011) s and 5/1024 (0.005) s, respectively. It should be noted that most RTHS systems run at 1/1024 (0.001) s, so any of these models will provide stable responses in a RTHS pretesting. Performance of the hyperbolic tangent model converges for normalized force RMS error at 1/2048 (0.0005) s while Bouc–Wen and algebraic dampers' performance converges when numerical integration time step is smaller than 1/1024 (0.001) s. The performance of viscous plus Dahl fluctuates till time step equal to 1/7168 (0.00014) s.

In terms of the speed, the algebraic model is the fastest one and viscous plus Dahl model closely follows. Hyperbolic tangent and Bouc–Wen model are slower, which is reasonable since algebraic and viscous plus Dahl models have much simpler equations modeling the force behavior. All of the damper models considered run in a sufficiently small time to be used in RTHS pretesting. While time is not critical here, if the structure model is larger or more MR damper models are used in the simulation, this may prove to be important consideration.

The accuracy of the viscous plus Dahl model is most sensitive to the changes of the numerical integration time step while the algebraic model is least sensitive to time step. The hyperbolic tangent and algebraic model appear to have better numerical accuracy in terms of normalized force RMS error at numerical time step equal to 1/1024 (0.001). Even when looking at the converged responses the results remain similar.

Each of the MR damper models presented in this paper demonstrates strengths and weaknesses in assisting in real-time hybrid simulation. Each of the models can be used in RTHS pretesting. This study has demonstrated the various limitations that should be considered when selecting a numerical model of a physical component in pretesting validation of RTHS, namely, stability and convergence, speed, and accuracy. Understanding the limitations of each of the damper models is important in selecting the specific model to be utilized in a particular real-time hybrid simulation.

Acknowledgments

The authors gratefully acknowledge the support of this research by the National Science Foundation under grants OISE-0612663, CMS-0612661, CMMI-0830173 and CMMI-0830235 and by the Joint Highway Research Advisory Council (JHRAC) of the University of Connecticut and the Connecticut Department of Transportation through the Connecticut Transportation Institute of the University of Connecticut under project JHRAC 08-6. The authors would like to thank the Lord Corporation for their generous support of this research; B F Spencer, Jr and B Phillips at Smart Structures Technology Laboratory at the University of Illinois at Urbana Champaign; and J Ricles, Y Chae and T Marullo at Lehigh University Network for Earthquake Engineering Simulation facility for their efforts conducting the real-time hybrid simulation. The authors would also like to thank F Ikhouane, J Rodellar and N Aguirre at Technical University of Catalunya, Spain for providing the viscous plus Dahl model in this study.

References

Aguirre N, Ikhouane F, Rodellar J and Christenson R E 2008 Modeling and identification of large scale magnetorheological dampers *4th European Conf. on Structural Control (St Petersburg)*

Bass B J and Christenson R E 2007 System identification of a 200 kN magneto-rheological fluid damper for structural control in large-scale smart structures *Proc. American Control Conf. (New York City, NY)* pp 2690–5

Bouc R 1971 Modèle mathématique d' hystérésis (a mathematical model for hysteresis) *Acustica* **21** 16–25

Carrion J E and Spencer B F 2006 Real-time hybrid testing using model-based delay compensation *Proc. 4th Int. Conf. on Earthquake Engineering (Taipei)* No 299

Carrion J E and Spencer B F 2007 Model-based strategies for real-time hybrid testing *Newmark Structural Engineering Laboratory Report Series* No. 6 University of Illinois at Urbana-Champaign, Urbana, IL

Chen C and Ricles J M 2009 Analysis of actuator delay compensation methods for real-time testing *Eng. Struct.* **31** 2643–55

Chen C, Ricles M J, Sause R and Christenson R E 2010 Experimental evaluation of an adaptive inverse compensation technique for real-time simulation of a large-scale magneto-rheological fluid damper *J. Smart Mater. Struct.* **19** 025017

Choi S, Lee S and Park Y 2001 A hysteresis model for the field-dependent damping force of a magnetorheological damper *J. Sound Vib.* **245** 375–83

Christenson R E and Lin Y Z 2008 Real-time hybrid simulation of a seismically excited structure with large-scale magneto-rheological fluid dampers *Hybrid Simulation Theory, Implementations and Applications* ed V E Saouma and M V Sivaselvan (London: Taylor and Francis) NL, ISBN: 978-0-415-46568-7

Christenson R E, Lin Y Z, Emmons A T and Bass B 2008 Large-scale experimental verification of semiactive control through real-time hybrid simulation *ASCE J. Struct. Eng.* **134** 522–35

Colgate J E, Stanley M C and Brown J M 1995 Issues in the haptic display of tool use *Int. Conf. Intelligent Robots and Systems* vol 3, p 3140

Dahl P R 1968 A solid friction model *Technical Report* The Aerospace Corporation, El Secundo, CA

Dahl P R 1976 Solid friction damping of mechanical vibrations *AIAA J.* **14** 1675–82

Dyke S J, Spencer B F, Sain M K and Carlson J D 1998 An experimental study of MR dampers for seismic protection *Smart Mater. Struct.* **7** 693–703

Dyke S J, Spencer B F, Quast P and Sain M K 1995 The role of control-structure interaction in protective system design *ASCE J. Eng. Mech.* **121** 322–38

Gamota D R and Filisko F E 1991 Dynamic mechanical studies of electrorheological materials: moderate frequencies *J. Rheol.* **35** 339–425

Gavin H P 2001 Multi-duct ER dampers *J. Intell. Mater. Syst. Struct.* **12** 353–66

Hakuno M, Shidawara M and Hara T 1969 Dynamic destructive test of a cantilever beam, controlled by an analog-computer *Trans. Japan Soc. Civil Eng.* **171** 1–9 (in Japanese)

Horiuchi T, Nakagawa M, Sugano M and Konno T 1996 Development of a real-time hybrid experimental system with actuator delay compensation *11th World Conf. on Earthquake Engineering* Paper No660

Housner G W, Soong T T and Masri S F 1994 Second generation of active structural control in civil engineering *Proc. 1st World Conf. on Structural Control (Pasadena, CA)* pp 3–18 (panel)

Jiang Z and Christenson R E 2010 200 kN hyperbolic tangent magneto-rheological fluid damper model with time varying inductance function *University of Connecticut Advanced Hazard Mitigation Laboratory Report* UConn-AHML-01-2010

Johnson E A, Ramallo J C, Spencer B F and Sain M K 1998 Intelligent base isolation systems *2WCSC: Proc. 2nd World Conf. on Structural Control (Kyoto)* vol 1, pp 367–76

Kennedy J and Eberhart R C 1995 Particle swarm optimization *Proc. IEEE Int. Conf. on Neural Networks (Perth)* (Piscataway NJ: IEEE Service Center) pp 1942–9

Kyrychko Y N, Blyuss K B, Gonzalez-Buelga A, Hogan S J and Wagg D J 2006 Real-time dynamic substructuring in a coupled oscillator-pendulum system *Proc. R. Soc.* **462** 1271–94

Lagarias J C, Reeds J A, Wright M H and Wright P E 1998 Convergence properties of the Nelder–Meade simplex method in low dimensions *SIAM J. Optim.* **9** 112–47

Mahin S A, Shing P B, Thewalt C R and Hanson R D 1989 Pseudodynamic test method—current status and future directions *J. Struct. Eng.* **115** 2113–28

MathWorks 2007 The MATLAB function reference online http://www.mathworks.com/access/helpdesk/help/techdoc/index.html?/access/helpdesk/help/techdoc/ref/fminsearch.html March 13

Nakashima M 2001 Development, potential, and limitations of real-time online (pseudo-dynamic) testing *Phil. Trans. R. Soc.* A **359** 1851–67

Park E, Lee S and Lee H 2008 Real-time hybrid testing of a steel-structure equipped with large-scale magneto-rheological dampers applying semi-active control algorithms *SMASIS2008: Proc. ASME 2008 Conf. on Smart Materials, Adaptive Structures and Intelligent Systems* pp 387–98, Paper no SMASIS2008-488

Phillips B, Chae Y, Jiang Z, Spencer B F, Ricles J, Christenson R, Dyke S J and Agrawal A 2010 Real-time hybrid simulation benchmark study with a large-scale MR damper *Proc. 5th World Conf. on Structural Control and Monitoring (Tokyo)*

Ruangrassamee A, Srisamai W and Lukkunaprasit P 2006 Response mitigation of the base isolated benchmark building by semi-active control with the viscous-plus-variable-friction damping force algorithm *J. Struct. Control Health Monit. Eng.* **13** 809–22

Shing P B, Nakashima M and Bursi O S 1996 Application of pseudodynamic test method to structural research *Earthq. Spectra* **12** 29–56

Song X, Ahmadian M and Southward S 2005 Modeling magnetorheological dampers with application of nonparametric approach *J. Intell. Mater. Syst. Struct.* **16** 421–32

Spencer B F, Dyke S J, Sain M K and Carlson J D 1997 Phenomenological model of a magnetorheological damper *ASCE J. Eng. Mech. Division* **123** 230–8

Spencer B F and Nagarajaiah S 2003 State of the art of structural control *J. Struct. Eng.* **129** 845–56

Spencer B F and Sain M K 1997 Controlling buildings: a new frontier in feedback *IEEE Control Syst. Mag.* **17.6** 19–35

Takanashi K 1975 Non-linear earthquake response analysis of structures by a computer actuator on-line system (part 1 details of the system) *Trans. Archit. Inst. Japan* **229** 77–83 (in Japanese)

Takanashi K and Nakashima M 1987 Japanese activities on on-line testing *J. Eng. Mech.* **113** 1014–32

Wen Y K 1976 Method of random vibration of hysteretic systems *ASCE J. Eng. Mech. Division* **102** 249–63

Wu B, Wang Q, Shing P B and Ou J 2007 Equivalent force control method for generalized real-timesubstructure testing with implicit integration *Earthq. Eng. Struct. Dyn.* **36** 1127–49

Yang G 2001 Large-scale magnetorheological fluid damper for vibration mitigation: modeling, testing and control *PhD Dissertation* University of Notre Dame